

Article

Simulations in the Topography Effects of Tianshan Mountains on an Extreme Precipitation Event in the Ili River Valley, China

Yufang Min ¹, Wanlong Huang ², Minjin Ma ^{2,*} and Yaonan Zhang ¹

¹ Northwest Institute of Eco-Environment and Resources, Chinese Academy of Sciences, Lanzhou 730000, China; myf@lzb.ac.cn (Y.M.); yaonan@lzb.ac.cn (Y.Z.)

² College of Atmospheric Sciences, Lanzhou University, Lanzhou 730000, China; huangwl19@lzu.edu.cn

* Correspondence: minjinma@lzu.edu.cn

Abstract: Xinjiang is located in an arid and semi-arid climate region in China, but Xinjiang Ili river valley is more humid, with higher precipitation intensity and precipitation, which is closely related to the role of the Tianshan Mountains. In this paper, through the NCRP $1^\circ \times 1^\circ$ reanalysis data and the conventional observation data of the Ili River Valley in Xinjiang, the terrain sensitivity experiment conducted by the WRF model is used to analyze the short-term extreme precipitation event of the Ili River Valley from 18–19 of May 2017, to reveal the influence of Tianshan Mountains on the extreme precipitation event of the Ili River Valley. The results show that: (1) The reduction or removal of the terrain will cause a wide range of wind field changes, weaken the vertical upward movement of the windward slope, and the accumulation of water vapor before the windward slope will also be reduced; a large-scale change of the terrain will also affect the direction of water vapor transportation. These effects together lead to a decrease or increase in regional precipitation. (2) “Fuzzy” (smooth) terrain will affect the precipitation simulated by changing the local vertical movement and water vapor transport, which shows that the WRF model’s accurate description of the terrain structure characteristics of mountainous areas is beneficial to accurately simulate the precipitation process on the windward slope area.

Keywords: Ili River Valley; numerical simulation; topography; precipitation



Citation: Min, Y.; Huang, W.; Ma, M.; Zhang, Y. Simulations in the Topography Effects of Tianshan Mountains on an Extreme Precipitation Event in the Ili River Valley, China. *Atmosphere* **2021**, *12*, 750. <https://doi.org/10.3390/atmos12060750>

Academic Editor: Daniel Argüeso

Received: 11 May 2021

Accepted: 4 June 2021

Published: 9 June 2021

Publisher’s Note: MDPI stays neutral with regard to jurisdictional claims in published maps and institutional affiliations.



Copyright: © 2021 by the authors. Licensee MDPI, Basel, Switzerland. This article is an open access article distributed under the terms and conditions of the Creative Commons Attribution (CC BY) license (<https://creativecommons.org/licenses/by/4.0/>).

1. Introduction

The most extreme precipitation events are inseparable from the interaction with terrain [1,2]. Terrain can trigger or change the precipitation process [3,4]. Since it is difficult to accurately describe the physical mechanism of mountainous areas, the misunderstanding of the various mechanisms of precipitation in mountainous areas may lead to errors in precipitation forecasts. Therefore, studies of the mechanism of short-term extreme precipitation events affecting mountain topography are crucial. Previous studies have shown that low-level wind is uplifted by terrain, which is conducive to generating terrain-enhanced precipitation [5,6]. Li et al. [7] believed that the obstruction of terrain has maintained the existence of a precipitation system for a long time, resulting in long-term heavy precipitation. The protrusion of the terrain and the overall structure will also change condensation with water vapor and thereby change the intensity and spatial distribution of precipitation [8]. However, the formative processes of topographic precipitation discussed previously appear to be diverse in different regions, especially in areas with more complex topography, which makes the research highly challenging.

Ili River Valley, China (42~45° N, 78~85° E), is located in the western part of Xinjiang, China, surrounded by Tianshan Mountains and is located in an arid and semi-arid climate region [9]. The Tianshan Mountains and the complex surrounding terrain play a key role in shaping this regional arid and semi-arid climate [10–15]. Due to the barrier effect of the Tianshan Mountains, a large amount of water vapor from the Mediterranean and Central Asia carried by the mid-latitude westerly wind is trapped in the Ili River Valley, and water

vapor is easy to accumulate in the Valley [16–18]. As a result, it has brought abundant water resources such as precipitation, snow and glaciers, and making the Ili River Valley a relatively humid area alienated from the surrounding areas, such as Central Asia and Northwest China. Therefore, a real “Oasis in the Desert” is formed between the arid and semi-arid zones [19,20]. In recent decades, in the context of climate change, precipitation in the Ili River Valley has shown an increasing trend, exceeding 5 mm/10a [21]. Besides, the spatiotemporal characteristics of the precipitation are constantly changing [22]. For example, the precipitation from 31 July to 1 August 2016 observed by the majority of meteorological stations broke through the extreme value in the history in the Ili River Valley. The 24 h cumulative precipitation was exceeded 100 mm at Gongliu in the Ili River Valley [17]. Record-breaking and more destructive precipitation events may have a higher probability of occurrence, which has a significant impact on the regional water cycle and ecological environment. To understand the mechanism and impact of terrain height and structure on precipitation well, numerical models are applied to study extreme precipitation events affected by the topography. The analysis and research of extreme precipitation events in the Ili River Valley, especially the impact of topography, can better serve the region’s economic construction, disaster prevention and mitigation [23,24].

This research is dedicated to analyzing a typical short-term extreme precipitation event in the Ili River Valley (18 May 2017–19 May 2017). Multiple stations in the Ili River Valley detected heavy rain during this extreme precipitation event (precipitation > 24 mm) [25]. The main goal of this paper is to (1) analyze the characteristics of this extreme precipitation event and explain the mechanism of this extreme precipitation event. (2) The topographical effect on this extreme precipitation event. (3) The effects of subtle changes in topographic structure or accurate topographic data on WRF model simulations in mountainous areas.

2. Data and Models

2.1. Data

The observational data used in this paper include conventional meteorological data (for example, 10 m wind direction and surface precipitation, etc.) from 10 meteorological stations (Figure 1b) in the Ili River Valley. The data are used for case analysis and verification of WRF model simulation results. NCRP FNL(Final) $1^\circ \times 1^\circ$ global tropospheric analysis and forecast grid sets are provided every 6 h (<https://rda.ucar.edu/datasets/ds083.2/index.html>, accessed on 7 June 2021) [26] for synoptic conditions analysis and WRF simulation. It is suitable for 32 levels from 1000 hPa to 10 hPa, including temperature, relative humidity, horizontal wind field, vertical movement, sea level pressure and other data.

2.2. WRF Model Configuration

The 2-day heavy precipitation process in the Ili area from 18 to 19 May 2017, is studied in this paper, using the Weather Research and Forecasting Model (WRF, version 4.0). The horizontal grid spacing of the model is 27 km, 9 km, and 3 km (Figure 1a). All regions use 34 vertical and horizontal layers, and the innermost layer (d03) covers the entire Ili area and Tianshan Mountains area (Figure 1b) with 322×193 grid points. Since the majority of water vapor from Central Asia and the Mediterranean Sea in the Ili River Valley, the outermost layer (d01) is shifted to the west of the study. The WRF model is simulated for 5 days, starting from 15 May 2017, the first 3 days are the mode start time, and the next 2 days are the parts required by the research. The physical parameterization scheme is set as WSM6 microphysical scheme, RTMM (Rapid Radiative Transfer Model) longwave radiation and Dudia shortwave radiation scheme, MYJ boundary layer scheme, Noah land surface scheme, BMJ convection parameterization scheme, and cumulus convection parameterization scheme, which is not used in WRF-d03.

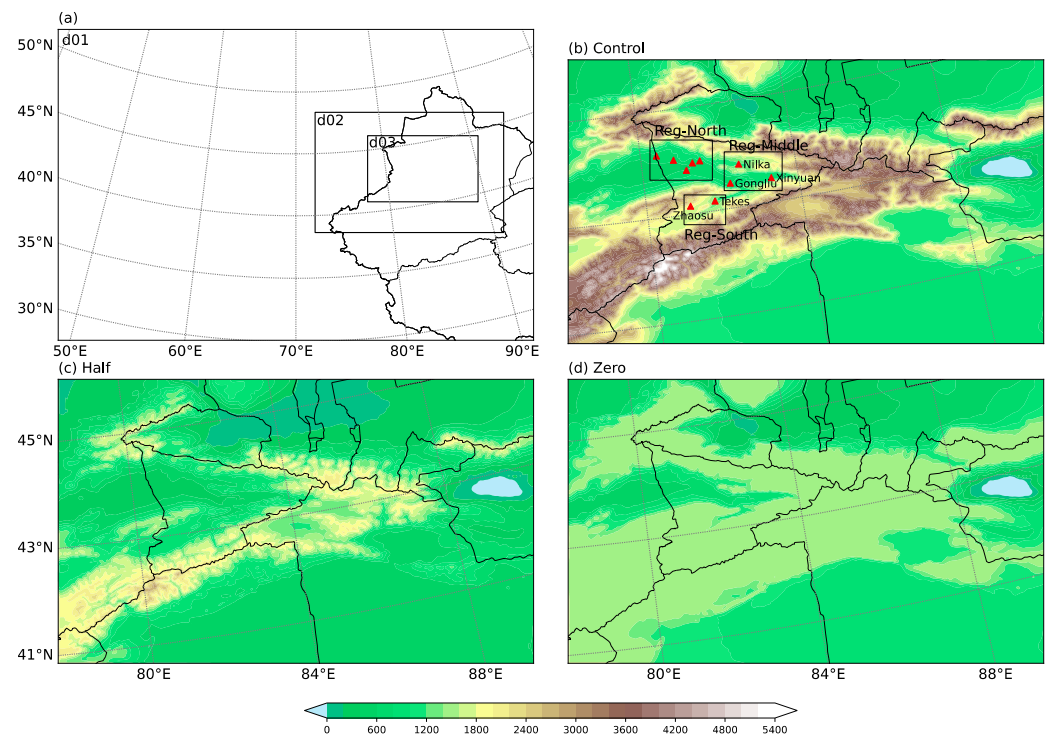


Figure 1. Numerical simulation domains. (a) The WRF triple nesting frame with d01, d02 and d03 areas, and the topography of the Ili River Valley in the d03 area of (b) Control, (c) Half, (d) Zero. The red triangle shows the location of the 10 meteorological stations in the Ili River Valley, and the black boxes are the three areas of the Ili River Valley.

Table 1 summarizes the parameterization scheme used in this study.

Table 1. A list of configuration settings for WRF.

Parameterisation	Option	Scheme
Microphysics	mp_physics = 6	WSM6
Longwave Radiation	ra_lw_physics = 1	RRTM
Shortwave Radiation	ra_sw_physics = 1	Dudhia
Land Surfaces	sf_surface_physics = 2	Noah Land Surface Model
Planetary Boundary layer	bl_pbl_physics = 2	MYJ
Cumulus	cu_physics = 2	Betts-Miller-Janjic
Parameterization	(d01, d02 only)	

2.3. Design of Terrain Sensitivity Experiment

In this article, considering that most extreme precipitation events are related to terrain, terrain sensitivity experiments have been conducted. The plan is shown in Table 2. The model terrain in the d03 is reduced by half (Half) (Figure 1c), removed (Zero), or smoothed (Smooth) (Figure 1d). The threshold of 1500 m is selected to remove the terrain because it is similar to the average altitude of the Ili area (d03 area), which can represent the average geographic background of the d03 area. By comparing the results of the control test and the sensitive test, the influence of the uplift of the entire Tianshan terrain on the wind field and the effect of water vapor transportation, and the influence of the terrain effect on the precipitation in the Ili River Valley can be analyzed.

In addition, the structural characteristics of the terrain will also affect the precipitation process in mountainous areas. Therefore, a five-point smoothing method is applied to the terrain for Smooth experiments. By comparing the results of the control test and the “fuzzy” terrain processing, the impact of subtle changes in terrain structure or more accurate terrain

data on the WRF simulation process can be analyzed. Figure 1c,d and Figure 2 show the d03 after the terrain changes.

Table 2. The topographic representation of the three sensitivity experiments.

Sensitivity Experiments	Scheme
Control	Real terrain
Half	Reduce the terrain in the d03 area to 0.5 times the original terrain
Zero	Reduce the terrain above 1.5 km in the d03 area to 1.5 km
Smooth	Smooth the terrain in the d03 area with five points

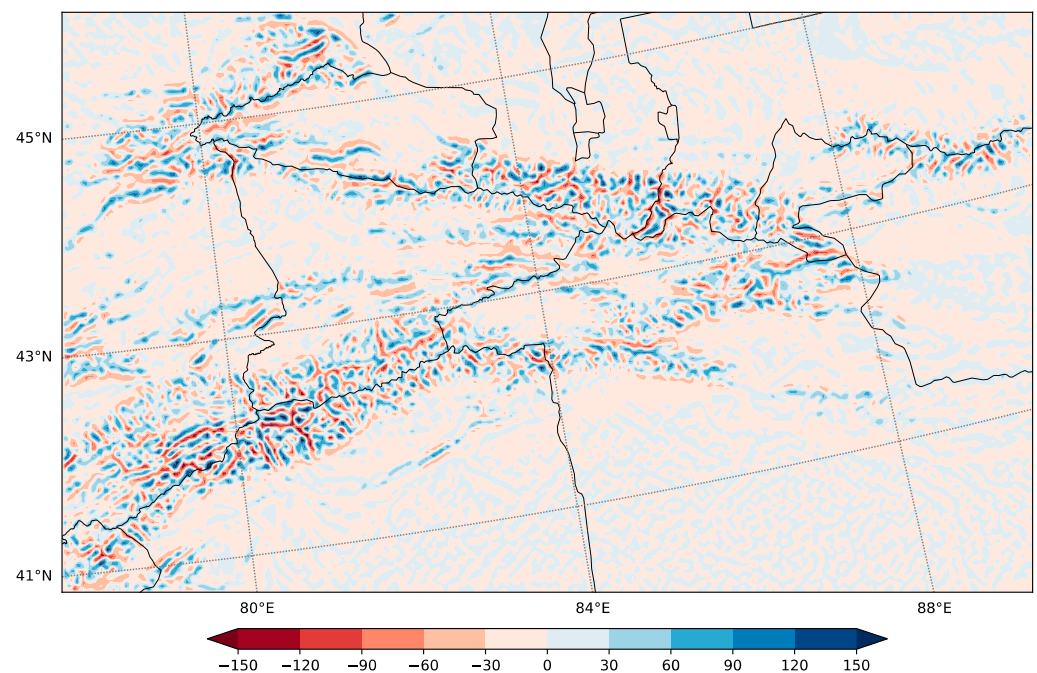


Figure 2. The altitude difference between the original terrain (Control) and the smoothed terrain (Smooth). Red represents the area where the terrain is lowered, and blue represents the area where the terrain is raised (unit: m).

3. Precipitation and Synoptic Conditions

An extreme precipitation event in the Ili River Valley from May 18 to 19, 2017 (UTC, the same below) was selected in this article for analysis. Among the meteorological stations in the Ili River Valley, there are five stations whose accumulative precipitation reached the rainstorm level of 24 mm within 24 h. The majority of meteorological stations had detected about seven rainfall processes with 24 h cumulative precipitation more than 24 mm in Ili River Valley from 2017 to 2018, and this extreme precipitation event was the most severe one in most meteorological stations' observation data. The precipitation process in the Ili River Valley began at 10:00 on May 18. From 10:00 to 15:00 on 18 May, the center of heavy precipitation was located in the southern mountain range of the Ili River Valley, the maximum cumulative precipitation at Zhaosu Station (81.13° E, 43.15° N) reached 10 mm at 3 h, but the average precipitation intensity at most stations in the valley with an altitude below 2 km was less than 1 mm/h. Subsequently, the heavy precipitation center moved to Gongliu County, Tekes County, and Xinyuan County, and the convection also moved to the northeast. Among them, the Tekes station (81.77° E, 43.18° N) had a maximum hourly precipitation intensity of 13.3 mm/h at 16:00 on the 18th. In addition, a new strong convective center was formed in the southern mountain range of the Ili River Valley. In Nilka County in the east of the Ili River Valley and Tekes County in the south, there were 3 h of accumulated heavy precipitation exceeding 20 mm. After 21:00 on 18 May, the impact

system gradually moved east again. The precipitation process in the southern part of the Ili Valley basically ended, and the precipitation process in the eastern region also basically ended at 03:00 on May 19. The rain belt movement of the extreme precipitation event is similar to the classification of eastward movement in the research of Li et al. [27], which is the majority of regional rainfall event's type in the Ili River Valley.

Figure 3 shows the circulation situation field in the upper and lower altitudes during this precipitation process using FNL $1^\circ \times 1^\circ$ Global tropospheric analysis and forecast grid sets. The 500 hPa mid-latitude circulation field during this precipitation is in the form of "two troughs and one ridge." There is a deep center of cold low pressure over the Black Sea at 00:00. The upper mid-latitude troposphere is dominated by westerlies (Figure 3a). The eastward movement of troughs and ridges in the 500 hPa latitude area weakened at 12:00, and the upper air is controlled by the southwest airflow. The trough front is conducive to the large-scale vertical ascending movement in the area, thereby providing this heavy precipitation favorable background conditions. For the low-altitude situation (Figure 3b,c), on the circulation diagrams of 700 hPa and 850 hPa, there are high-pressure ridges or warm high-pressure centers at 60°N – 70°N , and there is a northwesterly airflow north of Xinjiang, which is conducive to transporting cold air from Siberia to Ili River Valley. Beginning at 12:00 (Figure 3e,f), there is a warm and humid air current in the southwest of the Ili River Valley in Xinjiang, and there are strong westerlies over the Ili River Valley. Along with the convergence of airflow, and cold and warm advection converge, which is conducive to the generation of heavy precipitation. This circulation is continuously maintained before and during precipitation, which is conducive to continuously transporting water vapor and cold and warm air to the heavy precipitation zone, the enhancement of the vertical movement, the continuous occurrence and the development of convective systems.

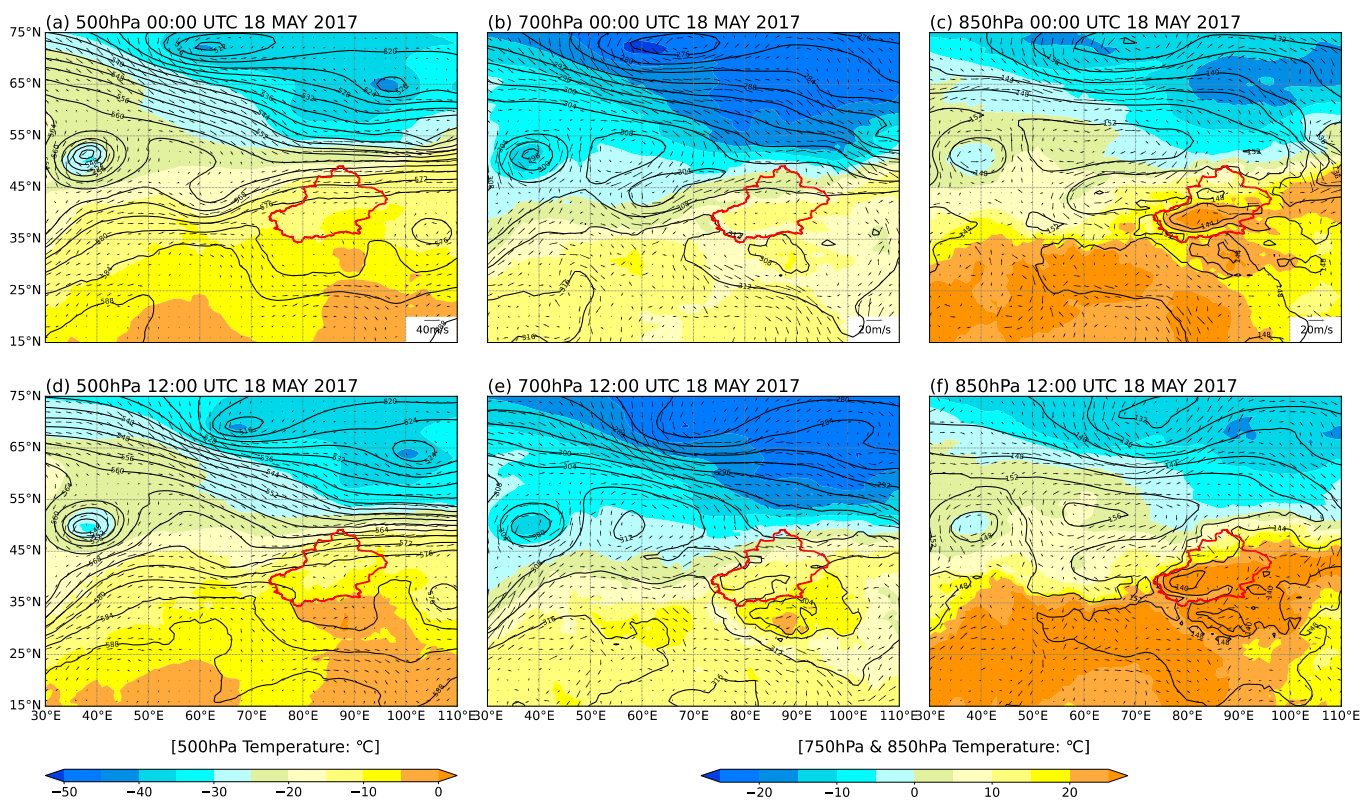


Figure 3. FNL reanalysis data for 500 hPa (left), 750 hPa (middle), and 850 hPa (right) geopotential height field (contour, unit: 10 gpm) at 00:00 (a–c) and 12:00 (d–f) on 18 May 2017; temperature (shadow) and wind field (arrow), the red line represents the Xinjiang region of China.

4. Simulation and Sensitivity Experiments

In this section, observation data and the results of the Control operation are compared to evaluate the accuracy of each element field characteristic and synoptic conditions simulated by the model at first. It is found that the Control experiment can accurately simulate the entire precipitation process. Subsequently, the topographical effects of extreme precipitation events are analyzed through the characteristics of each element (such as convective stability, water vapor flux, wind field, etc.). Finally, subtle changes in terrain structure or accurate terrain data are used to analyze the impact of WRF model simulation in mountainous areas.

4.1. Verification of Control Experimental Results

4.1.1. Precipitation

The Ili River Valley is a low-lying area around Tianshan Mountains. From the topography of Ili River Valley, as shown in Figure 1b, the Ili River Valley's west side is divided into two valleys by mountains, and the south valley is higher and narrower than the north valley. In order to study the influence of topography on this extreme precipitation, according to the terrain characteristics, the Ili River Valley is divided into three parts: the flat and relatively open northern (Reg-North), the middle (Reg-Middle), where the topography of the valley gradually narrows from west to east, and the southern valley (Reg-South) where the elevation is higher (Figure 1b).

Figure 4a is a comparison of the 48 h cumulative precipitation observed by 10 meteorological stations in the Ili area and the Control experimental results. Five meteorological stations of Reg-North are to the left of the blue line, and three meteorological stations of Reg-Middle are between the blue line and the red line, and two meteorological stations of Reg-South are to the right of the red line. The stations are from west to east in turn, and the specific locations are shown in Figure 3a (red triangle). The precipitation of the Reg-South and Reg-Middle regions during this extreme precipitation event was much higher than that of the Reg-North region. This was due to the fact that the valley topography of the Reg-South and Reg-Middle region was narrower and higher in altitude than that of the Reg-North region. In order to determine the accuracy of the WRF simulation of this precipitation process, the precipitation observed at 10 meteorological stations in the Ili River Valley was compared with the WRF simulation (Figure 4). The results of the WRF simulation have an underestimation of precipitation in the Reg-Middle region. The cumulative precipitation of 48 h is underestimated by about 38.9%. The underestimation of precipitation continues over time, and the period of heavy precipitation slightly lags behind the observation data (1–2 h), but overall, the trend of the precipitation process is basically consistent with the observation data (Figure 4c). During this precipitation process, the precipitation in Reg-North was small, and the duration was short. The simulation results also reflect such characteristics. For the Reg-South region, the accumulated precipitation simulated by WRF is basically the same as the observation data, and the accumulated precipitation error is about 3 mm. The intensity from 10:00 to 00:00, 18 May, in the simulation results are accurate, which is the beginning and ending time of the precipitation event. For all meteorological stations in the Ili River Valley, the correlation coefficient between the 48 h cumulative precipitation simulated by WRF and the observation data is 0.88, which passes the 99% confidence test, and the RMSE is 8.46 (Table 3). Figure 5 is the 3 h cumulative precipitation distribution of the WRF-d03 Control experiment and scatter plot of the Ili River Valley site. For the 3 h precipitation distribution in the Control experiment, the simulation results are basically consistent with the observations, except for the fact that it is 2–4 mm higher in the Reg-Middle area at 15:00–18:00. In short, although the WRF simulation results of hourly precipitation in the Reg-Middle area are different from the observation data, it still reflects the overall trend and characteristics of the precipitation process in the Ili River Valley to a certain extent.

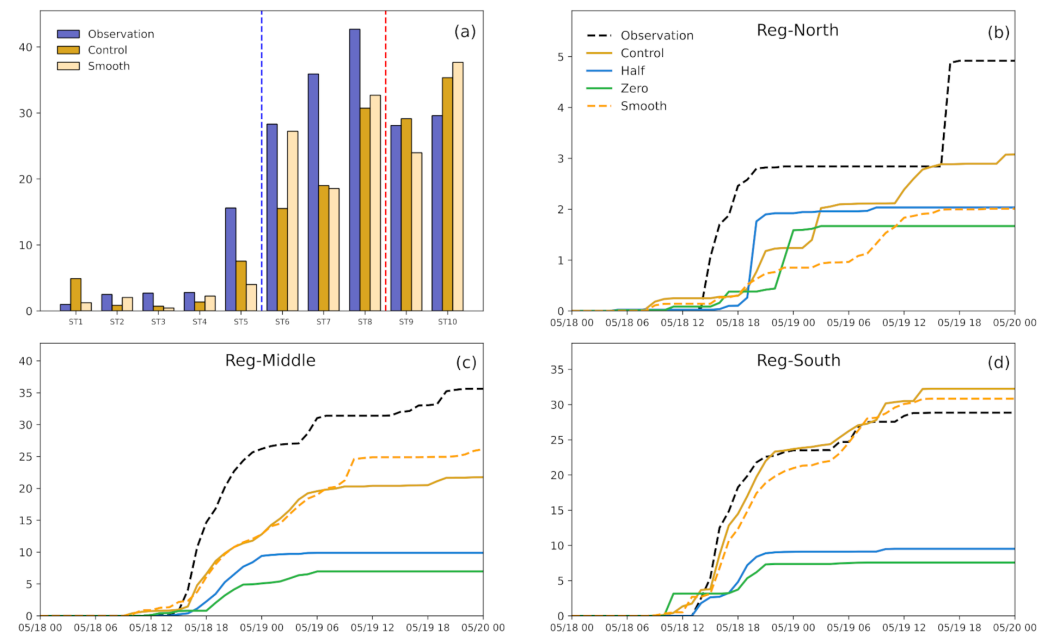


Figure 4. Control simulation and sensitivity experiments. (a) WRF-d03 output from the nearest grid point to the Ili River Valley meteorological station simulation Control experiment and Smooth experiment compared with the observation 48 h cumulative precipitation; the left side of the blue line is the station on the Reg-North; the blue line and red line is Reg-Middle; the red line on the right side is Reg-South, site direction in turn from west to east. Average cumulative precipitation (unit: mm) observed and simulated at the meteorological station at (b) Reg-North, (c) Reg-Middle, and (d) Reg-South.

Table 3. The statistical relationship between the observation conditions of various meteorological elements and the WRF-Control experiment.

Elements	Pearson Correlation	p-Value	RMSE
Precipitation	0.87798	0.00083	8.45833
Wind	0.54707	0.00878	2.85

4.1.2. Wind Simulation

In this heavy precipitation process, according to the observation of the wind field on the surface and the results of the Control experiment, during the whole precipitation period (10:00–03:00 on the 18th), the westerly wind in the Reg-North region was mainly stable and accompanied by strong winds over 10 m/s. The westerly wind did not change until the end of precipitation (Figure 6a–d). There was a counterclockwise wind field in the Reg-South area, and the lower troposphere swirl was conducive to the convergence of the wind field, forming an updraft (Figure 6c). Both the windward side and the leeward side of the Tianshan Mountains had large wind speed zones, especially at the end of the precipitation process, and the south side had a northerly wind greater than 20 m/s on the leeward side (Figure 6f). The correlation coefficient between the hourly wind field simulated by WRF and the observed wind field is 0.55, and it has passed the confidence level of 99%, and the RMSE is 2.85. The simulation of the wind field is generally consistent with the observation data.

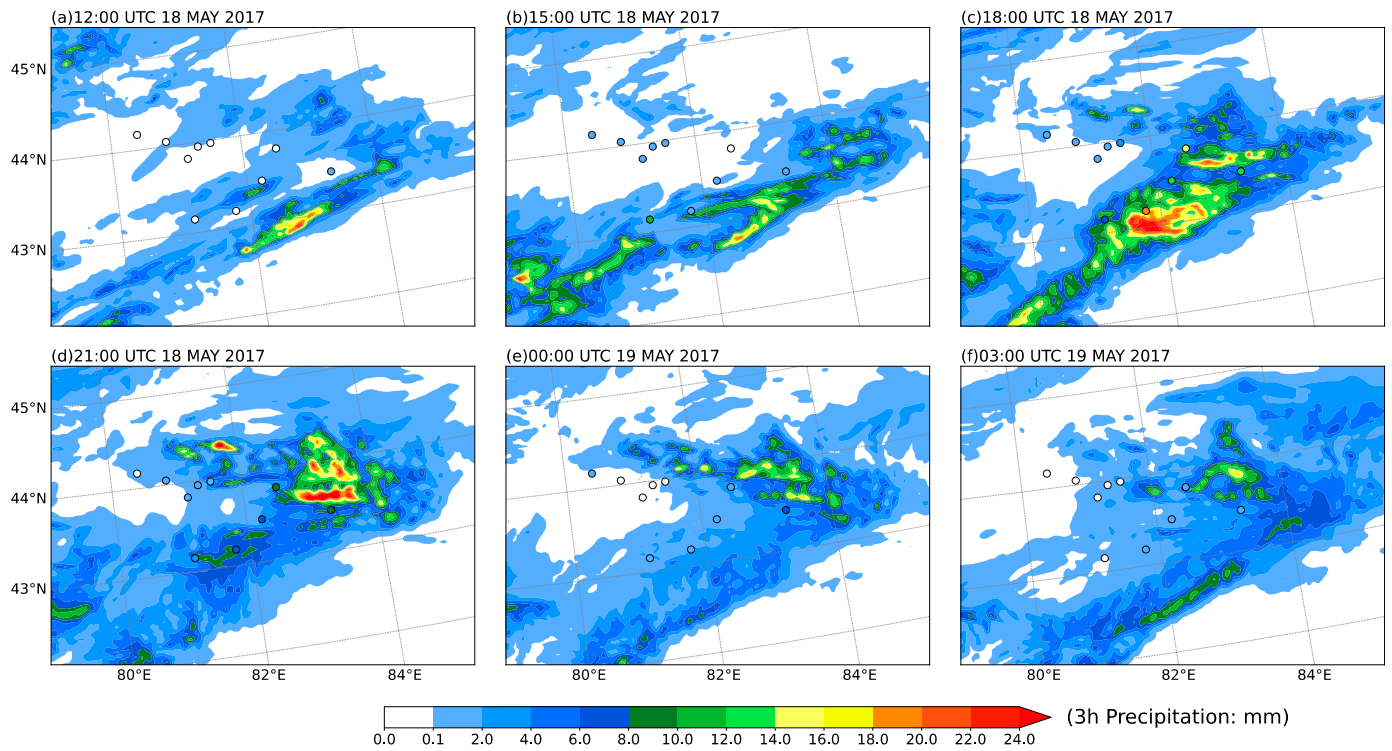


Figure 5. WRF-d03 Control experiment cumulative precipitation distribution and 3 h cumulative precipitation at meteorological stations in Ili River Valley, (a) 18 May 2017 12:00, (b) 18 May 2017 15:00, (c) 18 May 2017 18:00, (d) 18 May 2017 21:00, (e) 19 May 2017 00:00, and (f) 19 May 2017 03:00.

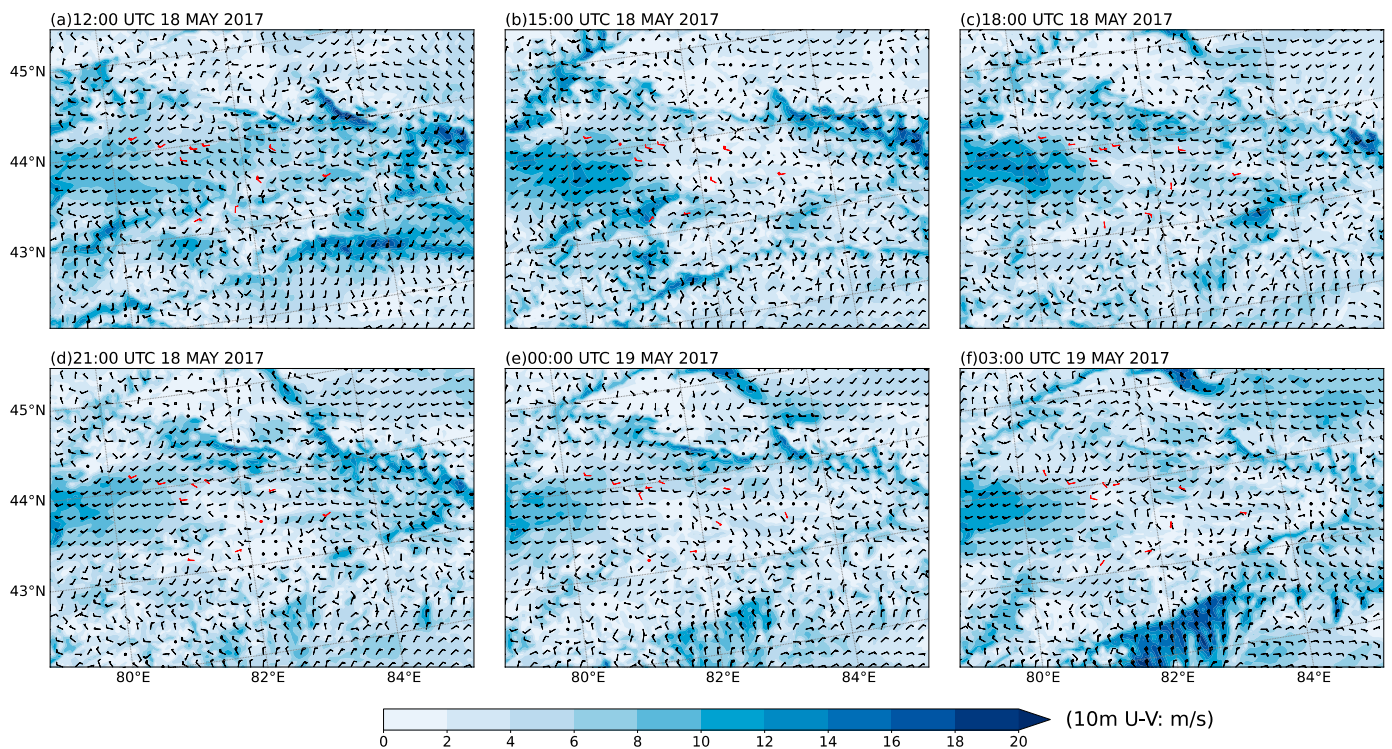


Figure 6. WRF-d03 Control experiment (black wind plume) and meteorological stations (red wind plume) wind direction and wind speed, blue shade is the wind speed of the Control experiment, (a) 18 May 2017 12:00, (b) 18 May 2017 15:00, (c) 18 May 2017 18:00, (d) 18 May 2017 21:00, (e) 19 May 2017 00:00, and (f) 19 May 2017 03:00.

In summary, the WRF-Control experiment can accurately reflect the characteristics of various meteorological elements in the precipitation process of the Ili River Valley. It shows that the configuration of the parameterization scheme in the terrain sensitivity experiment is reasonable, which can be used to better discuss the dynamic influence of the overall structure of the Tianshan Mountains on the precipitation in the Ili River Valley.

4.2. Topographic Effects

4.2.1. The Impact of Topographic Effects on Precipitation

Figure 7 shows the spatial distribution of the 48 h cumulative precipitation of the Control experiment in the Ili River Valley. The simulated precipitation is distributed along Tianshan Mountains. The higher the altitude, the higher the cumulative precipitation. The heavy precipitation centers of the Ili River Valley appear in the east and south of Ili. When the altitude is greatly reduced, the rainfall intensity corresponding to the Ili River Valley area is also greatly reduced, especially in the area where the original altitude is higher than 2000 m, and the area where the accumulated precipitation over 32 mm in 48 h basically disappears in the Control experiment. When the altitude is reduced by half (Half), the change in terrain height has little effect on the distribution of the precipitation belt in the Tianshan Mountains in the south of Ili. The precipitation belt distribution in the Reg-Middle area basically disappears, and the reduction of the terrain altitude has a particularly strong impact on the precipitation intensity significantly. The 48 h average cumulative precipitation in Reg-Middle and Reg-South regions decreased by 54.6% and 70.5%, respectively, and the cumulative precipitation of more than half of the stations in these two regions decreases by more than 1/2 (Table 4). After removing the topography of the Tianshan Mountains (Zero), the average cumulative precipitation in the Reg-Middle and Reg-South regions decreased by 68.0% and 76.6%, respectively, and the cumulative precipitation of 80% of the stations in the region drops by more than 2/3 (Table 4). This is caused by the weakening or disappearing vertical movement due to the weakening of the terrain uplift. It is worth noting that the region of the Tianshan Mountains corresponds with a higher amount of precipitation in the Zero simulation. It may be due to the fact that the zero simulation only removed the terrain above 2 km, and there is still a small topographic effect on the south slope of Tianshan Mountain. Besides, a free convergence might superimpose over the region. In addition, the precipitation period in Reg-Middle and Reg-South lags about 2 h (Figure 4c,d), which may also be caused by changes in the movement speed of the system that affect precipitation due to changes in terrain. However, for some stations in the Reg-North area with open and flat terrain, and for the experiment of greatly reducing the terrain height, there will be an increase in precipitation at individual stations. This may be due to the change in the wind field, the direction of water vapor transportation caused by the change in terrain and changes in the movement direction of the system that affects precipitation. Therefore, during this precipitation process, the Tianshan topography has an obvious effect on the increase and spatial alienation of the precipitation process.

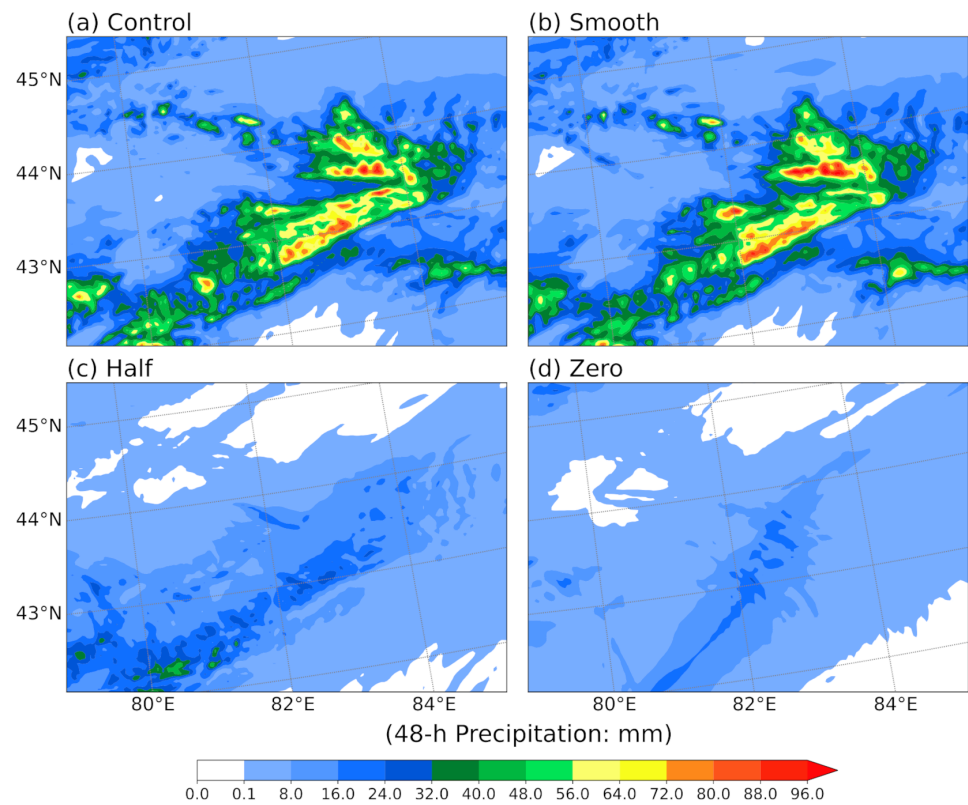


Figure 7. The distribution of 48 h cumulative precipitation in the WRF-d03 (a) Control, (b) Smooth, (c) Half, and (d) Zero.

Table 4. The ratio of 48 h cumulative precipitation and the Control experiment.

Experiment	Station									
	ST1	ST2	ST3	ST4	ST5	ST6	ST7	ST8	ST9	ST10
Smooth	0.25	2.38	0.65	1.67	0.53	1.75	0.98	1.06	0.82	1.07
Half	0.00	0.48	1.95	1.04	0.92	0.61	0.24	0.51	0.39	0.21
Zero	0.04	0.15	0.12	1.21	3.96	0.23	0.33	0.34	0.43	0.24

4.2.2. Analysis of Topographic Effects on the Cause of Heavy Rain

Because topographic precipitation is closely related to atmospheric water vapor content and unstable layer formation, it is important to analyze the mechanism of topographic effects on the enhancement of atmospheric water vapor transport and wind. In view of the fact that the Ili River Valley is dominated by zonal wind during this precipitation event, and the strong precipitation center has obvious characteristics along the zonal direction, the average latitude of the stations in the three regions of Reg-North, Reg-Middle, and Reg-South (43.99° N, 43.57° N, 43.17° N) is selected in this paper, and a vertical section along the zonal direction (80° E–84° E) is used to analyze the influence of terrain effects on this extreme precipitation (Figure 8).

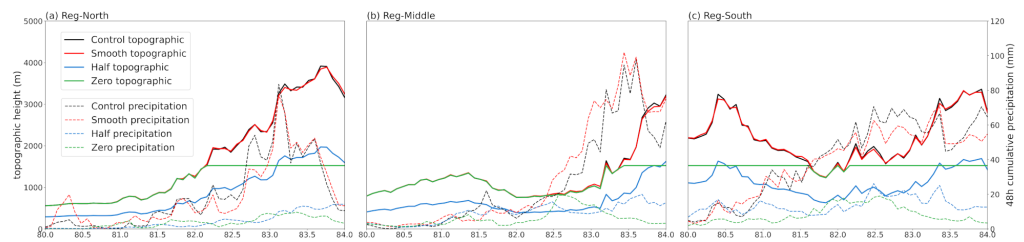


Figure 8. WRF-simulated topographic height (solid line, unit: m) and 48 h cumulative precipitation (dashed line, unit: mm) zonal vertical section of the average latitude of the control experiment and the sensitivity experiment in the 3 zones of d03, Including Control (black), Smooth (red), Half (blue), Zero (green), (a) the Reg-North area (43.99° N), (b) the Reg-Middle area (43.57° N), and (c) the Reg-South area (43.17° N).

Complicated terrain will affect the horizontal and vertical distribution of water vapor. Figures 9 and 10 show the water vapor fluxes (blue and red shades) at 12:00 on and 18:00, 18 May 2017, respectively. The Reg-North and Reg-Middle areas gradually increase in elevation from west to east. Additionally, the whole layer was dominated by westerly winds. There are windward slopes in the east of these areas. Due to the obstruction of the Tianshan Mountains, there is a large amount of water vapor accumulation near the surface and above the windward slope at 12:00 and 18:00 in the Tianshan Mountains (Figure 9a,b and Figure 10a,b). When the terrain height drops by half, a large amount of water vapor can directly across the mountains instead of accumulating near the surface layer before the windward slope. Water vapor flux decreases in front of windward slope and near the surface (Figure 9g,h,j,k and Figure 10g,h,j,k). The Reg-South area is surrounded by the Tianshan Mountains from north to south, and higher altitude in east and west and lower in the middle. At 12:00, the water vapor flux in the upper atmosphere is opposite to the water vapor flux in the lower layer. The water vapor flux in the upper layer is westward, and the lower layer is eastward. Because the topography of the valley is conducive to the accumulation of water vapor, there is a high-value area of water vapor flux in the middle of the Reg-South region (Figure 9c). When the elevation of the Reg-South area is reduced by half or the mountain terrain is removed, the high-value area of water vapor flux near the surface at 12:00 moves to the east and west sides and no longer appears in the middle area, even if there is a strong upward movement in the middle area at this time. However, in response to insufficient water vapor, it is difficult to form a heavy rainfall process (Figure 9i,l).

Complex terrain will affect the direction of water vapor transportation. At 12:00, the water vapor flux in the upper atmosphere of the Reg-North region increases in the west and decreases in the east (Figure 9g,j); at 18:00, the water vapor flux in the lower east of the Reg-South region increases (Figure 10i,l). Therefore, when the large-scale topography changes, the water vapor transport in the entire atmosphere changes. For example, after the terrain changes, the water vapor flux in the southern part of the Tianshan Mountains will increase significantly at 18:00 (Figure 11).

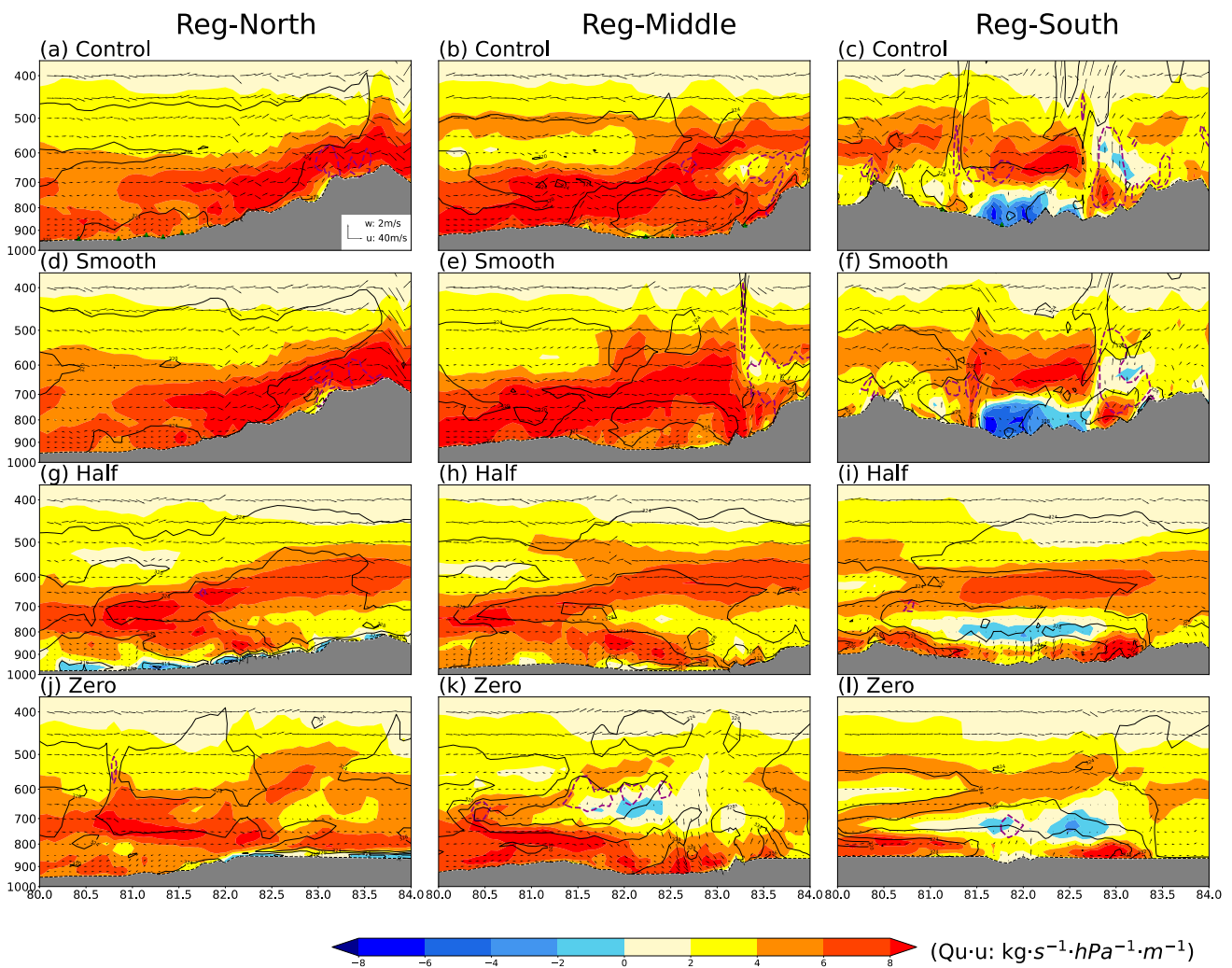


Figure 9. The zonal vertical profile of the average latitude of the control experiment and the sensitivity experiment in the 3 zones of the WRF simulation d03 at 12:00 on 18 May 2017, including the water vapor flux (red and blue shading), pseudo-equivalent potential temperature θ_{se} (black contour interval is 4 K, unit: K), cloud–water mixing ratio (purple contour, value 0.2 g/kg), u–w synthetic wind field (black wind vector, $w \times 20$, unit: m/s), terrain features (shaded gray). The left is the Reg-North area, the middle is the Reg-Middle area, and the right is the Reg-South area, (a–c) Control, (d–f) Smooth, (g–i) Half, and (j–l) Zero experiment.

Mountain terrain will produce strong vertical updrafts in the windward slope area, and strong ascending motion can trigger the release of unstable energy and cause convective instability. The stability of atmospheric junction can be expressed as the change of pseudo-equivalent potential temperature with height (θ_{se}). When the low-level pseudo-equivalent potential temperature decreases with height ($\partial\theta_{se}/\partial p > 0$), there is strong convective unstable stratification in the rainstorm area, and the strong vertical upward movement and a large amount of water vapor accumulation are conducive to the formation of water vapor condensation. These results are similar to Liu et al. [25] that the rapid development of vertical movement and convective instability in the lower atmosphere with the uplift of terrain are the reasons for the first heavy precipitation stage on the windward slope. At 12:00 and 18:00, the pseudo-equivalent equivalent potential temperature contours of the windward slopes are dense and decrease with height, which will produce a large cloud–water mixing ratio area, which provides favorable conditions for the outbreak of strong convective weather (Figure 9a,b and Figure 10a,b, purple dotted line). As the slope of the Tianshan Mountains decreases, the uplifting effect weakens, and the vertical upward movement also weakens. Meanwhile, the content of water vapor in the atmosphere also

changes with the change of terrain. The cloud–water mixing ratio becomes smaller or disappears corresponding to the large value area, and the precipitation intensity weakens (Figure 9g,h and Figure 10g,h).

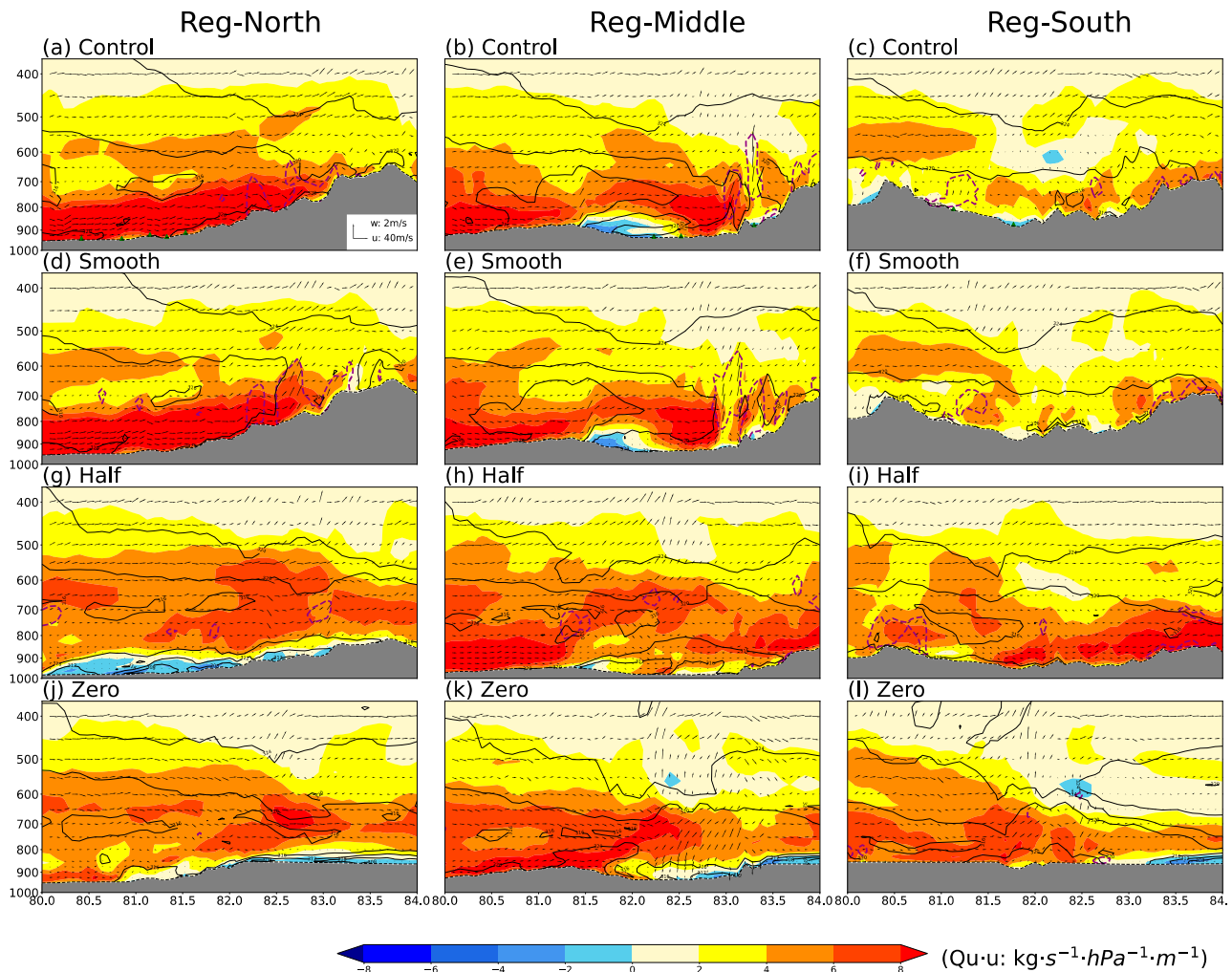


Figure 10. Time is 18:00 on 18 May 2017, the rest is the same as Figure 9. (a–c) Control, (d–f) Smooth, (g–i) Half, and (j–l) Zero experiment.

Therefore, vertical movement, water vapor content, and transportation are essential parts of cloud and precipitation in the WRF model. The values of these elements have changed significantly in these experiments of terrain change. This indicates that the vertical ascending motion and the content and transportation of water vapor in the atmosphere are strongly related to the terrain, and changes to local terrain will have a huge impact on local precipitation.

4.2.3. Impact of Smooth Terrain on Simulation Results

The terrain of the Tianshan Mountains in Ili River Valley is very complex, and even the 3 km resolution accuracy of the d03 area cannot accurately describe the features of the Tianshan terrain structure. Because topographic precipitation is closely related to atmospheric water vapor content and vertical movement, it is also important to predict future extreme precipitation events by analyzing the results of WRF simulation after a “fuzzy” representation of topographic characteristics.

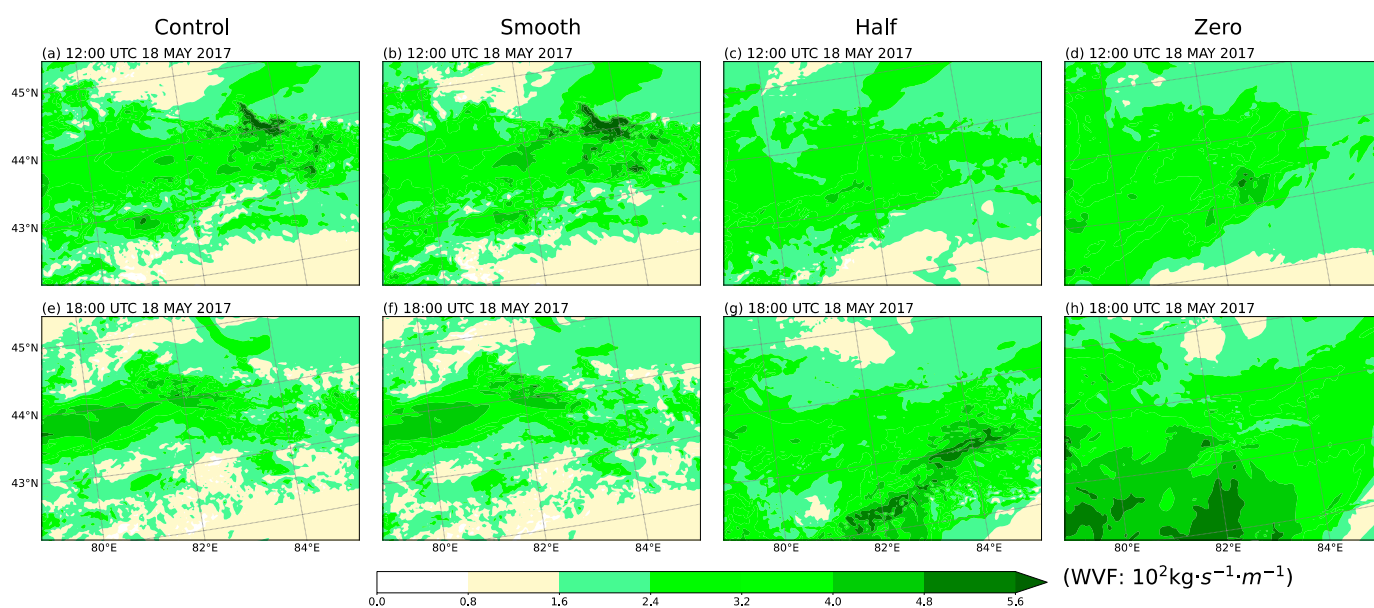


Figure 11. The whole layer of water vapor flux of WRF-d03 Control experiment and sensitivity experiment, from left to right are Control, Smooth, Half, and Zero experiment; (a–d) 18 May 2017 12:00 and (e–h) 18 May 2017 18:00.

When the terrain is smooth, the average 48 h accumulated precipitation of the stations in the Reg-North and Reg-South regions of the Smooth experiment decreases by 34.7% and 4.4%, respectively, and the Reg-Middle region increases by 20.3%. The results of the Smooth experiment simulation of cumulative precipitation in Reg-Middle and Reg-South regions are not so different from those of Control experiments, but for stations in the Reg-North region, the changes are large (Table 4). The east–west distribution characteristics of the 48 h cumulative precipitation in the three regions have basically not changed, but the local precipitation has changed, especially in the windward slopes of Tianshan Mountains. For example, in the Smooth experiment, the accumulated precipitation in the Reg-South windward slope area decreases by 8.1% compared with the Control experiment (Figure 8c), but the corresponding precipitation intensity south and north of Reg-South becomes stronger, and the range of the heavy precipitation center also expands (Figure 7b). The cumulative precipitation of Reg-North decreases by 12.4%, and the cumulative precipitation of the windward slope of the Reg-Middle area increases by 14.1% (Figure 8a,b). It can be seen that even small changes in the terrain will affect the intensity of local precipitation.

After the terrain is smoothed, the subtle changes of the underlying surface will basically not affect the upper atmosphere but will make the amplitude of the local terrain undulations smaller, thereby changing the vertical movement and water vapor distribution in the local area. For example, the whole layer of water vapor flux in the eastern part of the Ili River Valley in the Smooth experiment is larger than the Control experiment, but the central intensity will decrease accordingly (Figure 11a,b,e,f). In the Smooth experiment, the water vapor flux large value area in the Reg-South valley area is more widely distributed, the center intensity is weakened, and the intensity of the vertical ascending motion will also be weakened. The junction instability is weaker (Figure 10c,f). Under the combined effect of these influences, the rainfall intensity on the windward slopes of the mountains is lower. For the Reg-Middle area, even though the Smooth experiment has a relatively lower value of water vapor flux in the windward slope area compared to the Control experiment, the vertical upward movement area is wider, and the upward area is more westward (Figure 10e), so as a result, the amount of precipitation on the windward slopes in the area increases.

In summary, the “fuzzy” terrain can affect WRF-simulated precipitation by changing local vertical motion and water vapor transport, even by small changes. The area with

obvious precipitation change corresponds to the area with obvious terrain change, no matter the terrain altitude increases or decreases. As Wang et al. [2] point out, the simulations with high horizontal resolution or using the accurate dataset can increase the spatial consistency between the observed and simulated precipitation. This indicates that the accurate description of mountainous terrain structure is conducive to the accurate simulation of precipitation process by the WRF model in mountainous areas, especially in the windward slope area.

5. Conclusions and Discussion

FNL reanalysis data and site observation data from the Ili River Valley in Xinjiang, China, are selected in this paper and committed to analyzing the characteristics of a typical short-term extreme precipitation event in the Ili River Valley in Xinjiang, China (18 May 2017 to 19 May 2017). The terrain sensitivity experiments can be conducted further through the WRF model, aiming to obtain the topographic effect of this extreme precipitation event and subtle changes in topographic structure or the impact of accurate topographic data on the simulation of the WRF model in mountainous areas.

(1) The precipitation process in the Ili River Valley began at 10:00, May 18 and ended at 03: 00 on May 19. The maximum precipitation intensity occurred around 16:00, May 18. The center of heavy precipitation in this precipitation event appeared in the east and south of the Ili River Valley. It is flat and wide in the west of the Ili River Valley, with low precipitation. The precipitation process is mainly caused by the uplift of warm and humid air caused by the convergence of warm and cold advection in the Ili Valley.

(2) The reduction or removal of terrain will cause a wide range of wind field changes, weaken the vertical upward movement of the windward slope, and reduce the accumulation of water vapor in front of the windward slope, which will lead to the reduction of precipitation intensity and precipitation in the windward slope area. Large-scale changes to the terrain will also affect the direction of water vapor transportation, resulting in increased precipitation in flat areas where the precipitation was originally low.

(3) “Fuzzy” terrain will affect the precipitation of WRF simulation results by changing the local vertical movement and water vapor transportation. The main change area of precipitation appears in the place with higher smoothness (the place with greater altitude change). For mountainous areas, the accurate description of the structural characteristics of the WRF model is conducive to the accurate simulation of the precipitation process in the windward slope area.

In summary, topographic uplift will significantly enhance the precipitation process in the region. In the simulation process of WRF for mountainous regions, more accurate topographic data are used to describe the topographic structure of the region, which may be able to more accurately predict the precipitation intensity and precipitation in the region. In the subsequent work, Shuttle Radar Topography Mission (SRTM) data can be used to replace the original topographic dataset recommended by WRF for the simulation of plain or mountainous areas so as to better determine the impact of accurate terrain data on the simulation results.

Author Contributions: Conceptualization, M.M. and Y.M.; methodology, M.M. and W.H.; software, W.H.; validation, Y.M. and Y.Z.; formal analysis, W.H. and M.M.; investigation, W.H.; resources, Y.M.; data curation, Y.M.; writing—original draft preparation, W.H.; writing—review and editing, M.M. and Y.M.; visualization, W.H.; supervision, M.M.; project administration, Y.M. and M.M.; funding acquisition, Y.M. and M.M. All authors have read and agreed to the published version of the manuscript.

Funding: This research was funded by the National Key R&D Program of China, grant number 2017YFC1501805; Drought Meteorological Science Research Fund Project, grant number IAM202002; Plateau Atmosphere and Environment Key Laboratory of Sichuan Province, grant number PAEKL-2019-C3.

Institutional Review Board Statement: Not applicable.

Informed Consent Statement: Not applicable.

Data Availability Statement: Not applicable.

Acknowledgments: A lot of thanks are given to the National Cryosphere Desert Data Center, Lanzhou, China, which supplies precipitation data.

Conflicts of Interest: The authors declare no conflict of interest. The funders had no role in the design of the study; in the collection, analyses, or interpretation of data; in the writing of the manuscript, or in the decision to publish the results.

References

1. Houze, R.A. Orographic effects on precipitating clouds. *Rev. Geophys.* **2012**, *50*. [[CrossRef](#)]
2. Wang, Y.; Yang, K.; Zhou, X.; Chen, D.; Lu, H.; Ouyang, L.; Chen, Y.; Lazhu; Wang, B. Synergy of orographic drag parameterization and high resolution greatly reduces biases of WRF-simulated precipitation in central Himalaya. *Clim. Dyn.* **2020**, *54*, 1729–1740. [[CrossRef](#)]
3. Ntwali, D.; Ogwang, B.A.; Ongoma, V. The Impacts of Topography on Spatial and Temporal Rainfall Distribution over Rwanda Based on WRF Model. *Atmos. Clim. Sci.* **2016**, *6*, 145–157. [[CrossRef](#)]
4. Saha, U.; Singh, T.; Sharma, P.; Gupta, M.D.; Prasad, V.S. Deciphering the extreme rainfall scenario over Indian landmass using satellite observations, reanalysis and model forecast: Case studies. *Atmos. Res.* **2020**, *240*, 104943. [[CrossRef](#)]
5. Kang, Y.; Peng, X.; Wang, S.; Hu, Y.; Shang, K.; Lu, S. Observational analyses of topographic effects on convective systems in an extreme rainfall event in Northern China. *Atmos. Res.* **2019**, *229*, 127–144. [[CrossRef](#)]
6. Sarmadi, F.; Huang, Y.; Thompson, G.; Steven; Siems, T.; Manton, M.J. Simulations of orographic precipitation in the Snowy Mountains of Southeastern Australia. *Atmos. Res.* **2019**, *219*, 183–199. [[CrossRef](#)]
7. Li, H.; Wan, Q.; Peng, D.; Liu, X.; Xiao, H. Multiscale analysis of a record-breaking heavy rainfall event in Guangdong, China. *Atmos. Res.* **2020**, *232*, 104703. [[CrossRef](#)]
8. Basist, A.; Gerald, D.B.; Meentemeyer, V. Statistical Relationship between Topography and Precipitation Patterns. *J. Clim.* **1993**, *7*, 1305–1315. [[CrossRef](#)]
9. Huang, J.; Ma, J.; Guan, X.; Li, Y.; He, Y. Progress in Semi-arid Climate Change Studies in China. *Adv. Atmos. Sci.* **2019**, *36*, 922–937. [[CrossRef](#)]
10. Sato, T. Influences of subtropical jet and Tibetan Plateau on precipitation pattern in Asia: Insights from regional climate modeling. *Quat. Int.* **2009**, *194*, 148–158. [[CrossRef](#)]
11. Sun, J.; Gong, Z.; Tian, Z.; Jia, Y.; Windley, B. Late Miocene stepwise aridification in the Asian interior and the interplay between tectonics and climate. *Palaeogeogr. Palaeoclim. Palaeoecol.* **2015**, *421*, 48–59. [[CrossRef](#)]
12. Guo, L.; Li, L. Variation of the proportion of precipitation occurring as snow in the Tian Shan Mountains, China. *Int. J. Climatol.* **2015**, *35*, 1379–1393. [[CrossRef](#)]
13. Baldwin, J.; Vecchi, G. Influence of the Tian Shan on Arid Extratropical Asia. *J. Clim.* **2016**, *29*, 5741–5762. [[CrossRef](#)]
14. Sha, Y.; Shi, Z.; Liu, X.; An, Z.; Li, X.; Chang, H. Role of the Tian Shan Mountains and Pamir Plateau in Increasing Spatiotemporal Differentiation of Precipitation over Interior Asia. *J. Clim.* **2018**, *31*, 8141–8162. [[CrossRef](#)]
15. Shi, Z.; Sha, Y.; Liu, X.; Xie, X.; Li, X. Effect of marginal topography around the Tibetan Plateau on the evolution of central Asian arid climate: Yunnan–Guizhou and Mongolian Plateaux as examples. *Clim. Dyn.* **2019**, *53*, 4433–4445. [[CrossRef](#)]
16. Bothe, O.; Fraedrich, K.; Zhu, X. Precipitation climate of Central Asia and the large-scale atmospheric circulation. *Theor. Appl. Clim.* **2012**, *108*, 345–354. [[CrossRef](#)]
17. Zhong, Y.; Wang, B.; Zou, C.B.; Hu, B.X.; Liu, Y.; Hao, Y. On the teleconnection patterns to precipitation in the eastern Tianshan Mountains, China. *Clim. Dyn.* **2017**, *49*, 3123–3139. [[CrossRef](#)]
18. Zhou, Y.-S.; Xie, Z.-M.; Liu, X. An Analysis of Moisture Sources of Torrential Rainfall Events over Xinjiang, China. *J. Hydrometeorol.* **2019**, *20*, 2109–2122. [[CrossRef](#)]
19. Fan, X.; Liu, H.; Chen, X.; Wang, L. Effect of Sunny/Shady Slopes on Phases of Precipitation in China’s Tianshan Mountains. *Pol. J. Environ. Stud.* **2019**, *28*, 1651–1663. [[CrossRef](#)]
20. An, L.; Hao, Y.; Yeh, T.-C.J.; Zhang, B. Annual to multidecadal climate modes linking precipitation of the northern and southern slopes of the Tianshan Mts. *Theor. Appl. Clim.* **2020**, *140*, 453–465. [[CrossRef](#)]
21. Shi, X.; Xu, X. Interdecadal trend turning of global terrestrial temperature and precipitation during 1951–2002. *Prog. Nat. Sci.* **2008**, *18*, 1383–1393. [[CrossRef](#)]
22. Kutuzov, S.; Shahgedanova, M. Glacier retreat and climatic variability in the eastern Terskey–Alatoo, inner Tien Shan between the middle of the 19th century and beginning of the 21st century. *Glob. Planet. Chang.* **2009**, *69*, 59–70. [[CrossRef](#)]
23. Nuissier, O.; Ducrocq, V.; Ricard, D.; Lebeaupin, C.; Anquetin, S. A numerical study of three catastrophic precipitating events over southern France. I: Numerical framework and synoptic ingredients. *Q. J. R. Meteorol. Soc.* **2008**, *134*, 111–130. [[CrossRef](#)]
24. Houze, R.A.; Rasmussen, K.L.; Medina, S.; Brodzik, S.R.; Romatschke, U. Anomalous Atmospheric Events Leading to the Summer 2010 Floods in Pakistan. *Bull. Am. Meteorol. Soc.* **2011**, *92*, 291–298. [[CrossRef](#)]

25. Liu, J.; Zhou, Y.; Yang, L.; Zeng, Y.; Liu, W. The Instability and its Trigger Mechanism of Extreme Precipitation Event in the Yili River Valley on 31 July 2016. *Chin. J. Atmos. Sci.* **2016**, *43*, 1204–1218.
26. National Centers for Environmental Prediction; National Weather Service; National Oceanic and Atmospheric Administration; U.S. Department of Commerce. *NCEP FNL Operational Model Global Tropospheric Analyses, Continuing from July 1999*; Research Data Archive; National Center for Atmospheric Research: Boulder, CO, USA, 2000.
27. Li, L.; Li, J.; Yu, R. Characteristics of summer regional rainfall events over Ili River Valley in Northwest China. *Atmos. Res.* **2020**, *243*, 104996. [[CrossRef](#)]